YITP-05-31
OU-HET 533

The $H^{\pm}W^{\mp}Z^0$ vertex and single charged Higgs boson production via WZ fusion at the Large Hadron Collider

Eri Asakawa[1,*] and Shinya Kanemura[2,†]

[1] *Yukawa Institute for Theoretical Physics, Kyoto University, Kyoto 606-8502, Japan*

[2] *Department of Physics, Osaka University, Toyonaka, Osaka 560-0043, Japan*

Abstract

There is a variety of new physics scenarios which deduce extended Higgs sectors in the low energy effective theory. The coupling of a singly-charged Higgs boson ($H^{\pm}$) with weak gauge bosons, $H^{\pm}W^{\mp}Z^0$, directly depends on the global symmetry structure of the model, so that its experimental determination can be useful to test each scenario. We discuss predictions on this coupling in several models, such as the model with additional real and complex triplets, the Littlest Higgs model, the two Higgs doublet model and the minimal supersymmetric standard model. In order to measure the $H^{\pm}W^{\mp}Z^0$ coupling we consider single $H^{\pm}$ production via the WZ fusion mechanism at the CERN Large Hadron Collider. The production rate is hierarchically different among these models, so that this process can be useful to explore new physics scenarios.

PACS numbers: 12.60.Fr, 14.80.Cp

Keywords: Higgs, LHC, Beyond the Standard Model

*Electronic address: eri@yitp.kyoto-u.ac.jp

†Electronic address: kanemu@het.phys.sci.osaka-u.ac.jp

I. INTRODUCTION

Current precision data provide important indications for the structure of the electroweak symmetry breaking sector. In particular, the experimental value of the electroweak rho parameter (ρ) is very close to unity[1]. In the Standard Model (SM) with a scalar doublet field, this experimental requirement is automatically satisfied due to the custodial $SU(2)$ symmetry, by predicting the rho parameter to be exactly unity at the tree level. The data are then used to constrain the mass of the Higgs boson at the quantum level[2], which is the last undetermined parameter of the model. It is well known that the tree level prediction of $\rho = 1$ is a common feature of Higgs models with only doublets (and singlets)[3, 4]. In Higgs models with other $SU(2)$ representations such as triplets, the rho parameter is generally not unity at the tree level unless specific combinations are assumed among scalar multiplets. Although in such models the parameters are severely constrained by the rho parameter data, some new physics models would give a motivation to study phenomenology of these exotic representations.

In extended Higgs models, which would be deduced in the low energy effective theory of new physics models, additional Higgs bosons like charged and CP-odd scalar bosons are predicted. Phenomenology of these extra scalar bosons strongly depends on the characteristics of each new physics model. By measuring their properties like masses, widths, production rates and decay branching ratios, the outline of physics beyond the electroweak scale can be experimentally determined. The coupling of a singly-charged Higgs boson ($H^\pm$) with the weak gauge bosons, $H^\pm W^\mp Z^0$, is of particular importance for such an approach. Its magnitude is directly related to the structure of the extended Higgs sector under global symmetries[4, 5, 6]. It can appear at the tree level in models with scalar triplets, while it is induced at the loop level in multi scalar doublet models.

Models with scalar triplets may provide a solution for the origin of tiny neutrino masses. The triplet fields also appear in left-right symmetric models. The Littlest Higgs model[7, 8] and some extra dimension models[9] predict an additional complex triplet as well. The most discriminative feature of these triplet models is the prediction of both doubly- and singly-charged Higgs bosons[4]. In particular, detection of doubly charged Higgs bosons is a clear evidence for such exotic representations. On the other hand, there are lots of motivations to consider models with multi Higgs doublets, such as supersymmetry, topcolor[10], Little Higgs

models[11] and the model of gauge-Higgs unification[12]. Tiny neutrino masses (*e.g.* the Zee model[13]), and extra CP violating phases[14] which may be required for the realization of electroweak baryogenesis[15] also can be studied by introducing multi scalar doublets (plus singlets) in the electroweak scale. These multi doublet models predict singly-charged scalar bosons. To distinguish these extended Higgs models at collider experiments, the $H^{\pm}W^{\mp}Z^0$ vertex can be an useful probe.

At the Fermilab Tevatron with the proton-antiproton collision energy of 2 TeV, $H^{\pm}$ may be predominantly produced via the gauge boson associated production. They are expected to be produced via the gluon-bottom fusion at the CERN Large Hadron Collider (LHC) where incident protons collide with the energy of 14 TeV, assuming that they couple to quarks. Once a charged Higgs boson is produced, we may consider the decay into a $W^{\pm}Z^0$ pair as long as it is kinematically allowed. The decay rate of $H^{\pm} \to W^{\pm}Z^0$ has been evaluated in the minimal supersymmetric standard model (MSSM) and the two Higgs doublet model (2HDM) in Refs. [16, 17, 18], and also in the models with triplet Higgs fields in Ref. [19]. Impact of the $H^{\pm}W^{\mp}Z^0$ vertex on the physics with e^+e^- collisions has been studied in the triplet model[20]. Single $H^{\pm}$ production associated with a W boson, $e^+e^- \to H^{\pm}W^{\mp}$, may also be useful to study this vertex at a future linear collider[21, 22, 23, 24].

In this letter, we discuss the $H^{\pm}W^{\mp}Z^0$ vertex in various scenarios. Predictions on the form factors of the vertex are studied in models with the two doublet fields and also with triplets. We then consider testing the $H^{\pm}W^{\mp}Z^0$ coupling via single $H^{\pm}$ production in the WZ fusion process at the LHC. In general, Higgs boson production by vector boson fusion has advantages as compared to the other production processes, because the signal can be reconstructed completely and jet production is suppressed in the central region due to lack of color flow between the initial state quarks[25]. We evaluate the production rate of $pp \to W^{\pm *}Z^{0*}X \to H^{\pm}X$ with the effective $H^{\pm}W^{\mp}Z^0$ coupling in the effective vector boson approximation[26].

As the reference models, we here consider the model with a complex doublet with the hypercharge $Y = 1$, a real triplet ($Y = 0$) and a complex triplet ($Y = 2$)[27]; the Littlest Higgs model[7, 8, 28] where the low energy effective theory includes the SM-like Higgs doublet with an additional complex triplet with $Y = 2$; the general 2HDM; and the MSSM. These models predict different values for the production rate, so that each new physics scenario can be tested through the WZ fusion process at the LHC.

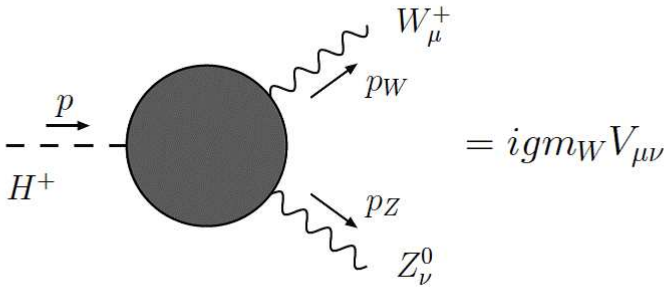

FIG. 1: The $H^\pm W^\mp Z^0$ vertex.

II. THE VERTEX

We here discuss general characteristics of the $H^\pm W^\mp Z^0$ coupling. The vertex (see Fig. 1) is defined as

$$igm_W V_{\mu\nu}\epsilon_W^{*\mu}(p_W,\lambda_W)\epsilon_Z^{*\nu}(p_Z,\lambda_Z), \tag{1}$$

where g is the weak gauge coupling, m_W is the mass of the weak boson $W^\pm$, and $\epsilon_V^{*\mu}(p_V,\lambda_V)$ ($V = W$ and Z) are polarization vectors for the outgoing weak gauge bosons with the momentum p_V and the helicity λ_V. The tensor $V_{\mu\nu}$ is decomposed in terms of three form factors as[16, 17, 18]

$$V_{\mu\nu} = Fg_{\mu\nu} + \frac{G}{m_W^2}p_{Z\mu}p_{W\nu} + \frac{H}{m_W^2}\epsilon_{\mu\nu\rho\sigma}p_Z{}^\rho p_W{}^\sigma, \tag{2}$$

where the antisymmetric tensor $\epsilon_{\mu\nu\rho\sigma}$ is defined so as to satisfy $\epsilon_{0123} = -1$. The values of F, G and H depend on the detail of the model. We discuss them in several models later.

The three form factors F, G and H in Eq. (2) respectively correspond to the coefficients f_{HWZ}, g_{HWZ} and h_{HWZ} of three operators in the effective Lagrangian,

$$\mathcal{L}_{\rm eff} = f_{HWZ}H^\pm W_\mu^\mp Z^\mu + g_{HWZ}H^\pm F_Z^{\mu\nu}F_{\mu\nu}^W + h_{HWZ}i\epsilon_{\mu\nu\rho\sigma}H^\pm F_Z^{\mu\nu}F_{\rho\sigma}^W + H.c., \tag{3}$$

where $F_{\mu\nu}^V$ ($V = W$ and Z) are the field strength tensors for weak gauge bosons. In Eq. (3), $H^\pm W_\mu^\mp Z^\mu$ is the dimension 3 operator while the rest two are dimension 5, so that only F may appear at the tree level. Models with triplet representations can predict the nonzero value of F at the tree level. On the other hand, in multi Higgs doublet models, the vertex is

induced only at the loop level because of the custodial $SU(2)$ symmetry in the kinetic term of the scalar doublet fields[6]. The one-loop contributions of the heavy particles in the loop to f_{HWZ}, g_{HWZ} and h_{HWZ} are described as

$$f_{HWZ} \sim \frac{g^2}{\cos\theta_W (4\pi)^2 v} M_i^2 \log M_i, \qquad g_{HWZ} \sim h_{HWZ} \sim \frac{g^2}{\cos\theta_W (4\pi)^2 v} \log M_i, \tag{4}$$

by using the power counting, where M_i represents the mass of the particle in the loop, θ_W is the Weinberg angle, and v ($\simeq$ 246 GeV) is the vacuum expectation value (VEV). Therefore, as long as the loop-induced vertex is substantial due to the dynamics of the loop particle, F gives the dominant contribution. This observation is correct for the quark loop contributions[17, 18], and for those of heavy Higgs bosons with the non-decoupling property where their masses are proportional to the VEV[18, 29].

The decay rate of $H^\pm \to W_i^\pm Z_i^0$, where $i = L$ represents the longitudinal polarization and $i = T$ does the transverse polarization, is expressed by

$$\Gamma(H^\pm \to W_i^\pm Z_i^0) = m_{H^\pm} \frac{\lambda^{1/2}(1, w, z)}{16\pi} |M_{ii}|^2, \tag{5}$$

where $\lambda(a, b, c) = (a - b - c)^2 - 4bc$, $w = (m_W^2/m_{H^\pm}^2)$ and $z = (m_Z^2/m_{H^\pm}^2)$. The longitudinal and transverse contributions are given in terms of F, G and H by

$$|M_{LL}|^2 = \frac{g^2}{4z} \left| (1 - w - z)F + \frac{\lambda(1, w, z)}{2w} G \right|^2, \tag{6}$$

$$|M_{TT}|^2 = g^2 \left\{ 2w|F|^2 + \frac{\lambda(1, w, z)}{2w} |H|^2 \right\}. \tag{7}$$

For the case of $m_{H^\pm} \gg m_Z$, we have $|M_{TT}|^2/|M_{LL}|^2 \sim 8m_W^2 m_Z^2/m_{H^\pm}^4$, so that the decay into a longitudinally polarized weak boson pair dominates that into a transversely polarized one. We use these formulas for the evaluation of the production rate of $pp \to W^{\pm *} Z^{0*} X \to H^\pm X$ in the effective vector boson approximation in Sec IV.

III. PREDICTIONS ON THE $H^\pm W^\mp Z^0$ VERTEX IN VARIOUS MODELS

A. Models with triplets

In models with triplets, the $H^\pm W^\mp Z^0$ vertex generally appears at the tree level. A common feature of the tree level contribution to the form factor F is the fact that it is proportional to the VEV of the triplet field[4, 27], $F \propto v'/v$, where v and v' represent the

VEVs of the doublet and the triplet in the model, respectively. When more than one triplet appear in the model, v' should be taken as the combination of the VEVs for them.

In general, models including a triplet field predict the value of the rho parameter not to be unity with the deviation proportional to v', so that v' in such models is strictly constrained to be much smaller than v; i.e., $F \ll 1$. For example, we consider the low energy effective theory of the Littlest Higgs model[7, 8], which predicts a complex triplet field in addition to the SM like doublet field. The Littlest Higgs model is the model with the $SU(5)$ global symmetry, with a locally gauged subgroup $G_1 \otimes G_2 = [SU(2)_1 \otimes U(1)_1] \otimes [SU(2)_2 \otimes U(1)_2]$. After the global $SU(5)$ symmetry breaks down to $SO(5)$ by the VEV of the order f, the $SU(5)$ 24 dimensional scalar field provides 14 degrees of freedom to the massless Goldstone bosons, which transform under the electroweak gauge symmetry as a real singlet, a real triplet, a complex doublet and a complex triplet. The degrees of freedom of the real singlet field and the real triplet are absorbed as the longitudinal components of the broken gauge groups. With the aid of the Coleman-Weinberg mechanism the remaining complex doublet and the complex triplet obtain their masses of orders v and f, respectively, and trigger the electroweak symmetry breaking. Therefore, an additional complex triplet field appears in the effective theory. The form factor F of the $H^{\pm}W^{\mp}Z^0$ coupling is given in this model by

$$F^{(\mathrm{LLH})} = \frac{4}{\cos\theta_W}\frac{v'}{v}. \tag{8}$$

The electroweak data indicate $1 \lesssim v' \lesssim 4$ GeV for $f = 2$ TeV[28]. The mass m_Φ of the triplet field Φ, of which $H^{\pm}$ is a component, is expressed at the leading order by[8]

$$m_\Phi^2 = \frac{2m_h^2 f^2}{v^2\left\{1 - (4v'f/v^2)^2\right\}}, \tag{9}$$

where m_h is the mass of the SM-like Higgs boson. We here consider the case with $m_h = 115$ GeV, $f = 1$ TeV (2 TeV), $v' = 5$ GeV (4 GeV), and $m_{H^{\pm}} = 700$ GeV (1.56 TeV) as a reference: i.e., the value of the form factor F is $|F^{(\mathrm{LLH})}|^2 \simeq 0.0085$ (0.0054).

In the model with additional real and complex triplet fields, the rho parameter can be set to be unity at the tree level, by imposing the custodial symmetry; i.e., $v'_{\mathrm{r}} = v'_{\mathrm{c}} (= v')$, where v'_{r} and v'_{c} are respectively the VEVs of the real and the complex triplet field[27, 30, 31]. After the electroweak symmetry breaking the remaining degrees of freedom is a five-plet ($H_5^{\pm}$), a three-plet ($H_3^{\pm}$) and two singlets under the custodial symmetry. In the case without mixing between the five-plet and three-plet, only the three-plet couples to fermions, while

the singly-charged Higgs boson $H_5^\pm$ of the five-plet couples to $W^\mp Z^0$. The form factor is given by[31]

$$F^{(\text{triplet})} = \frac{1}{\cos\theta_W}\sin\theta_H, \tag{10}$$

where $\sin\theta_H = \sqrt{8v'^2/(v^2+8v'^2)}$. In this model, the constraint from the rho parameter is weak and $\tan\theta_H$ can be taken to be of order 1. The strongest experimental bound on v'/v comes from the $Zb\bar{b}$ result. The limits at 95% CL are $\tan\theta_H \lesssim 0.5, 1$ and 1.7 for the mass of H_3 to be 0.1, 0.5 and 1 TeV, respectively[32]. We here take $\tan\theta_H$ to be 0.5 and m_{H_5}, the mass of charged Higgs boson from the five-plet, to be 200 GeV; i.e., $|F^{(\text{triplet})}|^2 \simeq 0.26$.

B. Multi Higgs doublet models

In models with multi Higgs doublets (and singlets), the $H^\pm W^\mp Z^0$ coupling is forbidden at the tree level[5] due to the custodial $SU(2)$ symmetry in the kinetic term of the scalar doublets. We here discuss the cases of the 2HDM and the MSSM[16, 17, 18]. The vertex can be induced at the one-loop level corresponding to the terms

$$\text{tr}\left[\tau_3(D_\mu\mathcal{M})^\dagger(D_\mu\mathcal{N})\right], \text{tr}\left[\tau_3\mathcal{M}^\dagger\mathcal{N}F_Z^{\mu\nu}F_{\mu\nu}^W\right], \text{and } i\epsilon_{\mu\nu\rho\sigma}\text{tr}\left[\tau_3\mathcal{M}^\dagger\mathcal{N}F_Z^{\mu\nu}F_W^{\rho\sigma}\right], \tag{11}$$

in the effective Lagrangian[18], according to the deviation from the custodial $SU(2)$ invariance in each part of the Lagrangian. In Eq. (11), $\mathcal{M}$ and $\mathcal{N}$ are 2×2 matrices defined by $\mathcal{M} = (i\tau_2\Phi^*, \Phi)$ and $\mathcal{N} = (i\tau_2\Psi^*, \Psi)$, where Φ and Ψ are the two scalar doublet fields in the gauge eigenstate basis[33]; i.e., $\langle\Phi\rangle = (0, v/\sqrt{2})^T$ and $\langle\Psi\rangle = 0$. Under $SU(2)_L\otimes SU(2)_R$, $\mathcal{M}$ and $\mathcal{N}$ transform as $\mathcal{M}\to g_L\mathcal{M}g_R^\dagger$ and $\mathcal{N}\to g_L\mathcal{N}g_R^\dagger$, where $g_{L,R}\in SU(2)_{L,R}$. It is clear that the terms in Eq. (11) are invariant under $SU(2)_L$, but not under $SU(2)_R$: i.e., the custodial symmetry is explicitly broken in these terms.

In the 2HDM, there are two sources to enhance the loop-induced form factors; i.e., the contribution from the top-bottom loop and those from the Higgs-boson loop. The large mass difference between top and bottom quarks indicates a large breakdown of the custodial $SU(2)$ symmetry in the top-bottom quark sector, and the loop induced $H^\mp W^\mp Z^0$ vertex can be sizable with quadratic power contributions of the top quark mass. The leading contribution can be extracted from the result of the full one-loop calculation[17] as

$$F^{(t-b\text{ loop})} \simeq \frac{N_c}{(4\pi)^2\cos\theta_W}\frac{m_t^2}{v^2}\cot\beta, \qquad \text{for } m_b \ll m_t, \tag{12}$$

where $\tan\beta$ is the ratio of VEVs of Higgs bosons[1]. Notice that this expression is independent of the type of Yukawa interaction, either Model I or Model II[4]. The values of $F^{(t-b\ \mathrm{loop})}$ are given by $F^{(t-b\ \mathrm{loop})} \simeq 0.01\cot\beta$; i.e., $|F^{(t-b\ \mathrm{loop})}|^2 \simeq 10^{-3}, 10^{-4}$ and 10^{-5} for $\tan\beta = 0.3, 1$ and 3, respectively. The value of $\tan\beta$ is bounded from below by the condition that the top Yukawa coupling should not be too large; i.e., $\tan\beta > 0.2 - 0.3$[21]. The one-loop diagrams of heavy neutral Higgs bosons can also contribute to this vertex when the mass difference between the charged Higgs boson and the CP-odd Higgs boson is large[18]. This mass splitting implies large breaking of the custodial $SU(2)$ symmetry under $\mathcal{M} \to g_L \mathcal{M} g_R^\dagger$ and $\mathcal{N} \to g_L \mathcal{N} g_R^\dagger$ in the Higgs potential. The constraint from the rho parameter can be satisfied by imposing "another" global $SU(2)$ symmetry under $\mathcal{M}_{21} \to g_L \mathcal{M}_{21} g_R^\dagger$, where $\mathcal{M}_{21} = [i\tau_2 \Phi_2^*, \Phi_1]$ in the Higgs potential[2]. The contribution of the Higgs boson loop can be important for $\tan\beta \gtrsim 3$, where the top-bottom loop contribution becomes suppressed because of the smaller Yukawa couplings[21]. However, too large mass splitting between the charged Higgs boson and the CP-odd Higgs boson causes a problem from the argument of perturbative unitarity[35, 36]. Consequently, contributions from the bosonic loop to F is constrained as $|F^{(\mathrm{bosonic\ loop})}|^2 \lesssim 10^{-5}$ for $3 \lesssim \tan\beta \lesssim 10$. Therefore, as the reference value of the 2HDM, we can take the value $|F^{(\mathrm{THDM})}|^2 \sim 10^{-3}$, 10^{-4} and 10^{-5} for $\tan\beta = 0.3$, 1 and $3 - 10$, respectively.

In the MSSM, the loop effect of super partner particles can enhance the vertex especially in the moderate values of $\tan\beta$, where the top-bottom loop contribution becomes suppressed. The new contributions become large according to the breakdown of global $SU(2)$ symmetry in the sfermion and chargino/neutralino sector. They can dominate the top-bottom loop contribution especially in the region of $\tan\beta \gtrsim 3$. However, the magnitude is at most

[1] If we consider the situation with $m_b \sim m_t$, the leading contribution is extracted for Model II 2HDM as[17]

$$F^{(t-b\ \mathrm{loop})} \simeq \frac{N_c}{(4\pi)^2 \cos\theta_W} \frac{m_t^2 - m_b^2}{3v^2} (\tan\beta + \cot\beta), \quad \text{if} \ \ m_b \sim m_t. \tag{13}$$

In the limit of $m_b \to m_t$, the leading contribution to F becomes zero, according that the Yukawa interaction for the third generation quarks is invariant under $SU(2)_L \times SU(2)_R$[6, 34]. This is described by expressing $\mathcal{L}_{\mathrm{Yukawa}}^{\mathrm{3rd\ gen.}} = \bar{Q}_L \mathcal{M}'_{21} Q_R$, where $Q_{L,R} = (t_{L,R}, b_{L,R})^T$ and $\mathcal{M}'_{21} = [i\tau_2 \Phi_2'^*, \Phi'_1]$ transform as $Q_{L,R} \to g_{L,R} Q_{L,R}$ and $\mathcal{M}'_{21} \to g_L \mathcal{M}'_{21} g_R^\dagger$ where $\Phi'_i = y_i \Phi_i$ $(i = 1, 2)$ with y_1 (y_2) to be the bottom (top) Yukawa coupling and $\Phi_{1,2}$ being the Higgs doublets and τ_i $(i = 1 - 3)$ being the Pauli matrix.

[2] The choice $m_{H^\pm} = m_H$ and $\sin(\alpha - \beta) = -1$, or $m_{H^\pm} = m_h$ and $\sin(\alpha - \beta) = 0$, corresponds to this case, where m_h and m_H are the masses of the lighter and heavier neutral CP-even Higgs boson, and α is the mixing angle between them.

$|F|^2 \sim 10^{-5}$[24], because of the decoupling property of super particles. On the other hand, as masses of the heavy Higgs bosons of the MSSM are approximately independent of the VEV and are nearly degenerate, the contribution from the Higgs-boson loop are small. Therefore, as a reference of the MSSM, we take $|F^{(\mathrm{MSSM})}|^2 \lesssim 10^{-5}$ for $\tan\beta \gtrsim 3$.

IV. SINGLE $H^\pm$ PRODUCTION VIA WZ FUSION AT THE LHC

Let us study the impact of the $H^\pm W^\mp Z^0$ vertex on the production cross section of $pp \to W^{\pm *} Z^{0*} X \to H^\pm X$ in the models discussed above. The vector boson fusion is a pure electroweak process with high-p_T jets going into the forward and backward directions from the decay of the produced scalar boson without color flow in the central region. The signal can be reconstructed, and the backgrounds are expected to be sufficiently reduced by appropriate kinematic cuts.

The hadronic cross section for $pp \to H^\pm X$ via WZ fusion is expressed in the effective vector boson approximation[26] by

$$\sigma_{\mathrm{eff}}(s, m_{H^\pm}^2) \simeq \frac{16\pi^2}{\lambda(1,w,z) m_{H^\pm}^3} \sum_{\lambda=T,L} \Gamma(H^\pm \to W_\lambda^\pm Z_\lambda^0) \tau \left.\frac{d\mathcal{L}}{d\tau}\right|_{pp/W_\lambda^\pm Z_\lambda^0}, \tag{14}$$

where $\tau = m_{H^\pm}^2/s$, and

$$\left.\frac{d\mathcal{L}}{d\tau}\right|_{pp/W_\lambda^\pm Z_\lambda^0} = \sum_{ij} \int_\tau^1 \frac{d\tau'}{\tau'} \int_{\tau'}^1 \frac{dx}{x} f_i(x) f_j(\tau'/x) \left.\frac{d\mathcal{L}}{d\xi}\right|_{q_i q_j/W_\lambda^\pm Z_\lambda^0}, \tag{15}$$

with $\tau' = \hat{s}/s$ and $\xi = \tau/\tau'$. Here $f_i(x)$ is the parton structure function for the i-th quark, and

$$\left.\frac{d\mathcal{L}}{d\xi}\right|_{q_i q_j/W_T^\pm Z_T^0} = \frac{c}{64\pi^4} \frac{1}{\xi} \ln\left(\frac{\hat{s}}{m_W^2}\right) \ln\left(\frac{\hat{s}}{m_Z^2}\right) \left[(2+\xi)^2 \ln(1/\xi) - 2(1-\xi)(3+\xi)\right], \tag{16}$$

$$\left.\frac{d\mathcal{L}}{d\xi}\right|_{q_i q_j/W_L^\pm Z_L^0} = \frac{c}{16\pi^4} \frac{1}{\xi} \left[(1+\xi)\ln(1/\xi) + 2(\xi-1)\right], \tag{17}$$

where $c = (v_W^2 + a_W^2)(v_Z^2 + a_Z^2)$, and

$$v_W = -a_W = \frac{g}{2\sqrt{2}}, \quad v_Z = \frac{g}{\cos\theta_W}\left(\frac{T_q^3}{2} - e_q \sin^2\theta_W\right), \quad a_Z = -\frac{g}{\cos\theta_W}\frac{T_q^3}{2}, \tag{18}$$

with T_q^3 and e_q to be the weak isospin and the electric charge for a quark q, respectively.

In evaluation for the cross section here, the contribution from the diagram with the effective $H^\pm W^\mp \gamma$ vertex is neglected. This may be justified by the fact that due to the

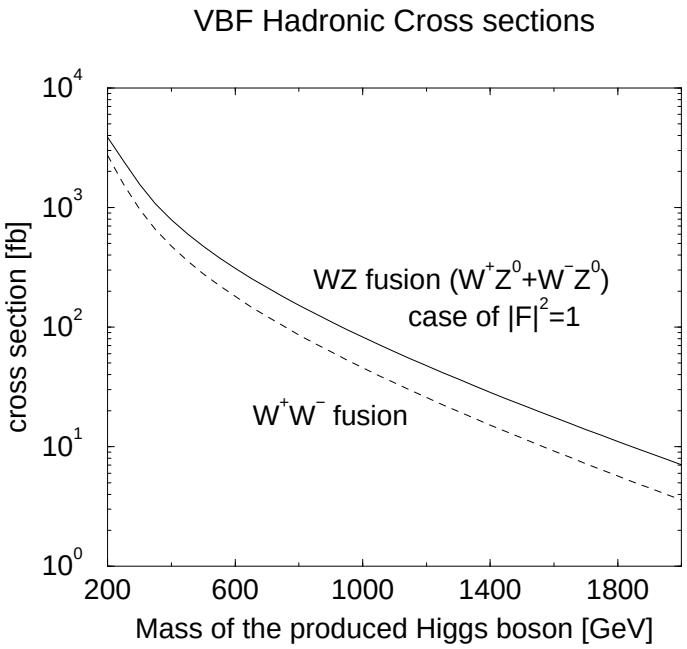

FIG. 2: The hadronic cross section of the $W^{\pm}Z^0$ fusion process and the W^+W^- fusion process as a function of the mass of the charged and neutral Higgs bosons, respectively. For the $W^{\pm}Z^0$ fusion, the form factor F is set to be unity. The SM prediction is shown for the W^+W^- fusion.

$U(1)_{\rm em}$ invariance there is no tree-level $H^{\pm}W^{\mp}\gamma$ coupling and loop-induced form factors of $H^{\pm}W^{\mp}\gamma$ do not have any quadratic mass contributions of the particles in the loop. Furthermore, for the $H^{\pm}W^{\mp}Z^0$ coupling the loop induced F can be much greater than the loop induced G and H in the multi doublet models: see Eq. (4). Consequently, the prediction for the cross section in each scenario can be obtained as $\sigma^{(\rm model)} \simeq |F^{(\rm model)}|^2 \times \sigma^{|F|^2=1}$ in a good approximation.

In Fig. 2, the hadronic cross section of $pp \to W^{\pm *}Z^{0*}X \to H^{\pm}X$ at the LHC ($\sqrt{s} = 14$ TeV) is shown as a function of $m_{H^{\pm}}$. The form factors F, G and H of the $H^{\pm}W^{\mp}Z^0$ vertex are set to be 1, 0 and 0, respectively. The hadronic cross section of SM Higgs boson production via W^+W^- fusion is also shown for comparison. CTEQ6L is used for the parton distribution function[37]. Because of a pp collider, the hadronic cross section for the W^+Z^0 fusion is about $1.5 - 2$ times greater than that for the W^-Z^0 fusion. The magnitude of $\sigma^{|F|^2=1}$ can be about 0.4×10^4 fb for $m_{H^{\pm}} = 200$ GeV. It decreases as $m_{H^{\pm}}$ grows, and becomes about 11 fb for $m_{H^{\pm}} = 1.8$ TeV. If we assume that $\sigma^{(\rm model)} = 1$ fb is a sufficient number to detect the signal, the required values of $|F^{(\rm model)}|^2$ are about 2.5×10^{-4}, 1.3×10^{-2}

and 10^{-1} for $m_{H^\pm} = 200$ GeV, 1 TeV and 1.8 TeV, respectively. In this case, 300 of $H^\pm$ are produced when $\sigma^{(\mathrm{model})} = 1$ fb at the LHC with the luminosity of 300 fb^{-1}.

In the model with additional real and complex triplets, $|F^{(\mathrm{triplet})}|^2$ can be of order 1. When $|F^{(\mathrm{triplet})}|^2 \simeq 0.26$, the cross sections are of order 1000 fb and 80 fb for $m_{H^\pm} = 200$ GeV and 600 GeV, respectively. In the Littlest Higgs model where the form factor F is given by $|F^{\mathrm{LLH}}|^2 \sim 0.0085$ (0.0054) for $f = 1$ TeV (2 TeV) with $m_{H^\pm} = 700$ GeV (1.56 TeV) the cross section can be about 2 fb (0.1 fb). In the 2HDM, the one-loop induced cross section can be of order $4, 0.4$ and 0.04 fb at $m_{H^\pm} = 200$ GeV, according to the values $|F^{(\mathrm{2HDM})}|^2 \sim 10^{-3}$, 10^{-4} and 10^{-5} for $\tan\beta = 0.3, 1$ and 3, respectively. In the MSSM, the values of $\tan\beta$ is bounded from below as $\tan\beta > 3 - 4$ by the LEP direct search result of the lightest Higgs boson[2]. As $|F^{(\mathrm{MSSM})}|^2 \lesssim 10^{-5}$ for $\tan\beta \gtrsim 3$, the cross section is at most 0.04 fb for $m_{H^\pm} > 200$ GeV.

The decay pattern of $H^\pm$ depends on the model. In the Littlest Higgs model in which $H^\pm$ couples to the top and bottom quarks, the main decay mode is expected to be a tb pair[8]. In the 2HDM and the MSSM, although there are potentially many decay modes, the main mode would also be the decay into a tb pair as long as it is kinematically allowed. In these cases, the signal would be $\ell\nu b\bar{b}$ ($\ell = e$ and μ). If the cross section is 1 fb, about 60 of the signal events are produced at the LHC with the luminosity of 300 fb^{-1}. The process can be completely reconstructed by using the information of the missing p_T and of the mass of $H^\pm$. The main backgrounds would come from $t\bar{t}$, $W + j$, WW and WZ, and their cross sections can be of order 1-10 pb. It is expected that appropriate kinematic cuts can reduce the backgrounds by 3-4 orders of magnitude by virtue of the distinct kinematic nature of vector boson fusion processes. By assuming a good efficiency (~ 0.25) for the double b tagging, the signal events would be detectable. On the other hand, in models with triplets that do not couple to fermions, it would mainly decay into a WZ pair. The model with a real and a complex triplets can correspond to this case. The signal event would be $\ell\ell\ell\nu$. For $\sigma^{(\mathrm{triplet})} \simeq 100$ fb, about 420 of the signal events are produced, assuming the luminosity of 300 fb^{-1}. Again, the process can be completely reconstructed. The main backgrounds would be $t\bar{t}$, $W + j$ and WZ in addition to the Drell-Yan process. We can expect that the backgrounds can be well rejected by the kinematic cuts, and that the signal can be detected[3].

[3] A feasibility study for this mode can be seen in the context of the Higgsless model in Ref. [38].

Needless to say that in either case, the feasibility study has to be performed by the realistic Monte Carlo simulation. This will be presented elsewhere[39].

V. CONCLUSIONS

We have discussed the $H^\pm W^\mp Z^0$ vertex in various physics scenarios. The magnitude of the $H^\pm W^\mp Z^0$ coupling directly depends on the global symmetry structure of the model, so that the experimental determination of the magnitude of the $H^\pm W^\mp Z^0$ coupling can be useful to test each scenario. The possibility of its measurement via single charged Higgs boson production by WZ fusion at the LHC has been discussed.

We have studied predictions on the $H^\pm W^\mp Z^0$ coupling in the model with additional real and complex triplets; the littlest Higgs model; the 2HDM; and the MSSM. These models predict hierarchical values for the form factor $F^{(\mathrm{model})}$. The cross section of $pp \to W^{\pm *} Z^0 X \to H^\pm X$ has been evaluated in terms of the effective $H^\pm W^\mp Z^0$ coupling in the effective vector boson approximation. In the models discussed in this letter (except for the MSSM), the cross section can exceed 1 fb: i.e., 300 of $H^\pm$ can be produced at the LHC for the luminosity of 300 fb^{-1}. By measuring this process we can obtain useful information to determine the structure of the Higgs sector, incorporating with a search for doubly charged Higgs bosons and that for single charged Higgs bosons via the other processes.

We have shortly discussed the signal for the cases where $H^\pm \to tb$ is dominant and where $H^\pm \to W^\pm Z^0$ is dominant. For the both cases, the backgrounds are expected to be considerably reduced because of the kinematic advantages in vector boson fusion. The more detailed study with the Monte Carlo simulation is in preparation.

Acknowledgments

The authors would like to thank Tomio Kobayashi for valuable discussions and comments, Kaoru Hagiwara, Mihoko Nojiri, Yasuhiro Okada, Eibun Senaha and Mayumi Aoki for useful discussions. A part of this work started in the discussion during the workshop "Physics in LHC era" at YITP, 13-15 December 2004 (YITP-W-04-20). S.K. was supported, in part, by Grants-in-Aid of the Ministry of Education, Culture, Sports, Science and Technology,

Government of Japan, Grant No. 17043008.

---

[1] S. Eidelman, et al., the Particle Data Group, Phys. Lett. B 592 (2004) 1.

[2] LEP Electroweak Working Group, *http://lepewwg.web.cern.ch/LEPEWWG/*.

[3] P. Sikivie, et al., Nucl. Phys. B 173 (1980) 189.

[4] J.F. Gunion, et al., *The Higgs Hunter's Guide*, Addison-Wesley, New York, 1990.

[5] J.A. Grifols, A. Méndez, Phys. Rev. D 22 (1980) 1725; A.A. Iogansen, N.G. Uraltsev, V.A. Khoze, *Sov. J. Nucl. Phys.* **36** (1982) 717.

[6] H.E. Haber, A. Pomarol, Phys. Lett. B 302 (1993) 435; A. Pomarol, R. Vega, Nucl. Phys. B 413 (1994) 3.

[7] N. Arkani-Hamed, et al., J. High Energy Phys. 07 (2002) 034.

[8] T. Han, et al., Phys. Rev. D 67 (2003) 095004.

[9] N. Arkani-Hamed, S. Dimopoulos, Phys. Rev. D 65 (2002) 052003; N. Arkani-Hamed, et al., Phys. Rev. D 61 (2000) 116003; E. Ma, U. Sarkar, Phys. Rev. Lett. 80 (1998) 5716.

[10] H.-J. He, C.T. Hill, T.M.P. Tait, Phys. Rev. D 65 (2002) 055006.

[11] N. Arkani-Hamed, et al., J. High Energy Phys. 08 (2002) 021; M. Schmaltz, Nucl. Phys. Proc. Suppl. 117 (2003) 40.

[12] Y. Hosotani, S. Noda, K. Takenaga, Phys. Lett. B 607 (2005) 276.

[13] A. Zee, Phys. Lett. B 161 (1985) 141; S. Kanemura, et al., Phys. Rev. D 64 (2001) 053007; D.A. Dicus, H.-J. He, J.N. Ng, Phys. Rev. Lett. 87 (2001) 111803; Phys. Lett. B 536 (2002) 83.

[14] S. Weinberg, Phys. Rev. Lett. 37 (1976) 657.

[15] A.G. Cohen, D.B. Kaplan, A.E. Nelson, *Annu. Rev. Nucl. Part. Sci.***43** (1993) 27; A.T. Davies, et al., Phys. Lett. B 336 (1994) 464; K. Funakubo, A. Kakuto, K. Takenaga, Prog. Theor. Phys. 91 (1994) 341; J.M. Cline, K. Kainulainen, A.P. Vischer, Phys. Rev. D 54 (1996) 2451; S. Kanemura, Y. Okada, E. Senaha, Phys. Lett. B 606 (2005) 361.

[16] T.G. Rizzo, Mod. Phys. Lett. A 4 (1989) 2757; A. Méndez, A. Pomarol, Nucl. Phys. B 349 (1991) 369; J.L. Díaz-Cruz, J. Hernández-Sánchez, J.J. Toscano, Phys. Lett. B 512 (2001) 339.

[17] M. Capdequi Peyranére, H.E. Haber, P. Irulegui, Phys. Rev. D 44 (1991) 191.

[18] S. Kanemura, Phys. Rev. D 61 (2000) 095001.

[19] K. Cheung, D.K. Ghosh, J. High Energy Phys. 0211 (2002) 048.

[20] K. Cheung, R. Phillips, A. Pilaftsis, Phys. Rev. D 51 (1995) 4731; R.M. Godbole, B. Mukhopadhyaya, M. Nowakowski, Phys. Lett. B 352 (1995) 388; D.K. Ghosh, R.M. Godbole, B. Mukhopadhyaya, Phys. Rev. D 55 (1997) 3150.

[21] S. Kanemura, Eur. Phys. J. C 17 (2000) 473.

[22] S.-H. Zhu, hep-ph/9901221; A. Arhrib, et al., Nucl. Phys. B 581 (2000) 34.

[23] S. Kanemura, S. Moretti, K. Odagiri, J. High Energy Phys. 02 (2001) 011.

[24] H.E. Logan, S. Su, Phys. Rev. D 66 (2002) 035001; Phys. Rev. D 67 (2003) 017703.

[25] S. Asai, et al., Eur. Phys. J. C 32S2 (2004) 19.

[26] G. Kane, W. Repko, W. Rolnick, Phys. Lett. B 148 (1984) 367; M. Chanowiz, M.K. Gaillard, Phys. Lett. B 142 (1984) 85; S. Dawson, Nucl. Phys. B 249 (1985) 42.

[27] P. Galison, Nucl. Phys. B 232 (1984) 26; H. Georgi, M. Machacek, Nucl. Phys. B 262 (1985) 463; R. Chivukura, H. Georgi, Phys. Lett. B 182 (1986) 181.

[28] M.-C. Chen, S. Dawson, Phys. Rev. D 70 (2004) 015003.

[29] P. Ciafaloni, D. Esprin, Phys. Rev. D 56 (1997) 1752; S. Kanemura, T.-A. Tohyama, Phys. Rev. D 57 (1998) 2949; S. Kanemura, et al., Phys. Rev. D 70 (2004) 115002.

[30] M. Chanowitz, M. Golden, Phys. Lett. B 165 (1985) 105.

[31] J. Gunion, R. Vega, J. Wudka, Phys. Rev. D 42 (1990) 1673; Phys. Rev. D 43 (1991) 2322.

[32] H. Haber, H. Logan, Phys. Rev. D 62 (2000) 015011.

[33] H. Georgi, *Had. J. Phys.* **1** (1978) 155.

[34] M. Veltman, *Acta Phys. Pol.* **B 8** 475 (1977); Phys. Lett. B 70 (1977) 253; M. Einhorn, J. Wudka, Phys. Rev. D 39 (1989) 2758; Phys. Rev. D 47 (1993) 5029.

[35] B.W. Lee, C. Quigg, H.B. Thacker, Phys. Rev. D 16 (1977) 1519.

[36] H. Hüffel, G. Pocsik, *Z. Phys.* C **8**, 13 (1981); J. Maalampi, J. Sirkka, I. Vilja, Phys. Lett. B 265 (1991) 371; S. Kanemura, T. Kubota, E. Takasugi, Phys. Lett. B 313 (1993) 155; A. Akeroyd, A. Arhrib, E.-M. Naimi, Phys. Lett. B 490 (2000) 119; I.F. Ginzburg, I.P. Ivanov, hep-ph/0312374.

[37] J. Pumplin, et al., J. High Energy Phys. 0207 (2002) 012.

[38] A. Birkedal, K. Matchev, M. Perelstein, Phys. Rev. Lett. 94 (2005) 191803.

[39] E. Asakawa, S. Kanemura, in preparation.